

High Q^2 -Anomaly at HERA and Supersymmetry

H. Dreiner¹ and P. Morawitz²

¹ Rutherford Lab., Chilton, Didcot, OX11 0QX, UK

² Imperial College, HEP Group, London SW7 2BZ, UK

Abstract

We discuss the recently observed excess of high Q^2 neutral current deep inelastic scattering events at HERA in the light of supersymmetry with broken R-parity. We find more than one possible solution. We consider the possibilities for testing these hypotheses at HERA, the TEVATRON and at LEP. One lepton-number violating operator can account for both the HERA data and the four-jet anomaly seen by ALEPH at LEP.

1 Introduction

Recently both experiments at HERA have quoted an excess at high Q^2 in their neutral current deep inelastic scattering (NC DIS) data [1, 2]. For $Q^2 > 15,000 \text{ GeV}^2$, *H1* have found 12 events where they expect ≈ 5 from the Standard Model (SM) [1]. For $Q^2 > 20,000 \text{ GeV}^2$ *ZEUS* observe 5 events where they expect ≈ 2 from the SM [2]. In addition, *H1* have seen a slight excess in their charged current deep inelastic scattering (CC DIS) [1]. Due to the low rate, we find it is still too early to comment on this. The NC DIS discrepancies could be the first hint of physics beyond the SM [3]. There have been three main suggestions predicting an excess of events at high Q^2 at HERA: contact interactions [4], leptoquarks [5], and supersymmetry with broken R-parity [6, 7, 8].

Contact interactions are a parametrisation of unknown physics at a higher energy via gauge-invariant but non-renormalisable operators. For HERA, these are dimension-6 $eeqq$ operators. They can lead to an increase or a depletion of high Q^2 events depending on the sign of a free-parameter. These events should not show any peak-like structure. With the low-energy (well below the new scale) data one can attempt to extract the unknown scale of the new physics. This analysis should be performed on the HERA data but we do not further consider this possibility here.

Both leptoquarks and supersymmetry with broken R-parity predict s-channel resonances in positron-proton scattering. Within supersymmetry, we expect new states between 100 GeV and 1 TeV in order to maintain the solution to the gauge hierarchy problem [9]. Many models also predict leptoquarks, but most of them involve heavy leptoquarks beyond present experimental reach. In the following, we shall thus focus on the implications of the recent HERA data for supersymmetry with broken R-parity. However, due to the equivalence of a leptoquark and the R-parity violating Yukawa coupling, large parts of our discussion apply to both. When relevant we shall emphasise below where the two descriptions diverge.

In Section (2) we briefly review supersymmetry with broken R-parity and focus on the relevant terms for HERA. In Section (3) we review the indirect bounds on these operators. In Section (4) we then determine which R-parity violating operators could possibly lead to the observed excess at HERA while still being consistent with the existing indirect bounds. In Sections (5) through (7) we discuss how these operators could be tested in future runs at HERA, as well as with present and upcoming data at LEP and at the TEVATRON. In Section (8) we present our conclusions. In the appendix we have collected some of the relevant formula for completeness.

2 Supersymmetry with Broken R-Parity at HERA

When minimally extending the particle content of the SM to incorporate supersymmetry one must add an extra Higgs $SU(2)_L$ doublet and then double the particle content. The most general interactions of these particles consistent with supersymmetry and $SU(3)_c \times$

$SU(2)_L \times U(1)_Y$ gauge symmetry are those of the minimal supersymmetric standard model (MSSM) [10] as well as the superpotential terms¹[12]

$$\lambda_{ijk} L_i L_j \bar{E}_k + \lambda'_{ijk} L_i Q_j \bar{D}_k + \lambda''_{ijk} \bar{U}_i \bar{D}_j \bar{D}_k. \quad (1)$$

Here L (Q) is the lepton (quark) doublet superfield, and \bar{D}, \bar{U} (\bar{E}) are the down-like and up-like quark (lepton) singlet superfields, respectively. $i, j, k = 1, 2, 3$ are generation indices. The last two sets of terms in (1) lead to rapid proton decay [13]. The solution of this problem in the MSSM is to impose R-parity,

$$R_p = (-1)^{3B+L+2S}, \quad (2)$$

a multiplicative discrete symmetry. Here B denotes baryon number, L lepton number² and S the spin of a field. All SM fields have $R_p = +1$; their supersymmetric partners have $R_p = -1$. This solution is not unique. There are many models which protect the proton but allow a subset of the terms in (1) [11, 14, 15]. This subset can be as small as two operators even for a gauge symmetry [14]. All these alternative solutions are denoted “R-parity violation”. In the following, we shall focus on the subset of the operators (1)

$$\lambda'_{1jk} L_1 Q_j \bar{D}_k. \quad (3)$$

At HERA these operators can lead to resonant squark production

$$e^+ + \bar{u}_j \rightarrow \tilde{d}_k, \quad (4)$$

$$e^+ + d_k \rightarrow \tilde{u}_j. \quad (5)$$

This was first proposed by J. Hewett in Ref.[6] where she considered the direct R-parity violating decay of the squark to the initial state. The processes (4,5) were discussed in more detail in [7, 8] where the squark cascade decays via a photino were included. This enables the distinction from a leptoquark, depending on the supersymmetric spectrum. The full mixing in the neutralino sector was first considered in [16] for R-parity violation at HERA. For a scalar top quark ($j = 3$), the decays via the neutralino are kinematically forbidden. This scenario was discussed in considerable detail by T. Kon *et al.* [17]. The squark decays for the full gaugino mixing including the chargino were discussed by E. Perez [18] and in a shorter version in [19]. This enabled a full classification of the final state topologies at HERA.

Making use of all this work, we wish to determine the size and generation structure j, k of the coupling λ'_{1jk} of (3) which is preferred by the HERA data. We would also like to consider the best estimate for the squark mass. However, in order to do that we must first consider the indirect bounds on the couplings λ'_{1jk} .

¹There is the further term $\kappa_i L_i H_u$ which violates lepton number. If the soft-breaking terms are universal it can be rotated away [11].

²This should not lead to any confusion with the lepton doublet superfield, L , of Eq.(1).

λ'_{111}	λ'_{112}	λ'_{113}	λ'_{121}	λ'_{122}	λ'_{123}	λ'_{131}	λ'_{132}	λ'_{133}
0.001 ^(a)	0.05 ^(b)	0.05 ^(b)	0.06 ^(c)	0.06 ^(d)	0.01 ^(d)	0.06 ^(c)	0.01 ^(d)	0.002 ^(d)
0.004	0.11	0.11	0.13	0.087	0.014	0.13 ^(c)	0.014	0.003

Table 1: Indirect bounds on first lepton generation operators $LQ\bar{D}$. The first line is the bound for a scalar fermion mass of $100\,GeV$ the second line for $210\,GeV$. The bounds derive from the following physical processes: ^(a) neutrinoless double beta decay [20], ^(b) charged current universality [21, 22], ^(c) atomic parity violation [23, 22], and ^(d) ν_e mass [24]. The bounds from ^(b) and ^(c) scale linearly with the squark mass $(\tilde{M}_{\tilde{q}}/100)\,GeV$. The bound from ^(d) scales with the square root $\sqrt{\tilde{M}_{\tilde{q}}/100\,GeV}$. The bound ^(a) scales as $(\tilde{M}_q/100\,GeV)^2\sqrt{\tilde{M}_{\tilde{q}}/100\,GeV}$. In the Table we have conservatively estimated the gluino mass at $\tilde{M}_{\tilde{g}} = 1\,TeV$.

3 Previous Indirect Bounds

The operators (3) can contribute to several processes with initial and final state SM particles via the exchange of virtual sleptons or squarks. Since to date all such processes have been observed in agreement with the SM, this leads to upper bounds on all the couplings which we summarise in Table 1. We give the bounds for a scalar fermion mass of $100\,GeV$, which is the standard, and $210\,GeV$, which is what we require below. These two bounds are related via scaling properties which are explicitly given in the table caption. The bounds are all well below the electromagnetic coupling. The bounds from atomic parity violation (^(c)) are more strict than those in Ref.[21] since they incorporate more recent data [23, 22]. The bounds from the mass of the electron neutrino have previously not been extended to all the couplings. It is straightforward to do this using the equations of Ref.[24]. There are also limits from direct searches for supersymmetry with broken R-parity which are not competitive [25]. As we discuss below, the bounds from direct leptoquark searches can be re-interpreted in this context and are competitive. However, they are more model dependent.

4 HERA's high Q^2 excess interpreted as s-channel squark production

4.1 R-parity Violating Squark Decays

We would now like to interpret the observed excess at HERA in terms of supersymmetry with R-parity violation. For this, we combine the *H1* and *ZEUS* data in order to compare it more easily with different R-parity violating models. For $Q^2 > 20,000\,GeV$ *H1* and *ZEUS* see a total of 10 events [1, 2], where 4.08 ± 0.36 events are expected from SM contributions [26]. The total integrated luminosity of the two experiments is $34.3\,pb^{-1}$, which translates into an excess cross-section over the SM expectation of

$$\sigma_{ex}(Q^2 > 20,000\,GeV) = (0.17 \pm 0.07(stat))\,pb. \quad (6)$$

In Figures 1 and 2 we show this combined excess cross section as a horizontal band.

The combined reconstructed values of the hypothetical squark mass $M_{\tilde{q}}$ (where $M_{\tilde{q}}$ is related to Bjorken-x by $M_{\tilde{q}}^2 = xs$ and s is the centre-of-mass energy squared) show some spread between the two experiments ($M_{\tilde{q}} = 200\,GeV$ for $H1$, $M_{\tilde{q}} = 220\,GeV$ for $ZEUS$). Simply combining the two experiments, we obtain

$$M_{\tilde{q}} = (210 \pm 20)\,GeV, \quad (7)$$

as our best estimate.

In order to determine the contribution from R-parity violation we consider one of the operators (3) at a time while assuming the others are negligible. For a given non-vanishing operator $\lambda'_{1jk} L_1 Q_j \bar{D}_k$, the produced \tilde{u}_j , or \tilde{d}_k squark can have many decay modes, depending on the mass spectrum of the supersymmetric particles [7, 8, 18, 19, 27]. For all SUSY spectra, the squark can decay via the operator itself resulting in the interactions

$$e^+ + \bar{u}_j \rightarrow \tilde{\bar{d}}_k \rightarrow e^+ + \bar{u}_j, \quad (8)$$

$$e^+ + \bar{u}_j \rightarrow \tilde{\bar{d}}_k \rightarrow \bar{\nu} + \bar{d}_j, \quad (9)$$

$$e^+ + d_k \rightarrow \tilde{u}_j \rightarrow e^+ + d_k, \quad (10)$$

at HERA. The first and third have equivalent initial and final states to NC DIS and can thus contribute to the observed excess. Analogously, the second can contribute to CC DIS. Let us for now assume these are the only decay modes of the produced \tilde{u}_j or \tilde{d}_k squark. We then compute the production cross section using [6, 8] and the MRS-G structure functions [28]. For (8) and (9) we include the extra contribution to the width for the other decay mode. We also include the interference term between the new contribution and the SM contribution.

In Figure 1, we plot the production cross section $\sigma(e^+ + d_k \rightarrow \tilde{u}_j \rightarrow e^+ + d_k)$ for $Q^2 > 20,000\,GeV$ as a function of the R-parity violating couplings λ'_{1j1} , λ'_{1j2} , λ'_{1j3} , respectively. For each coupling, the three curves are for the squark masses $M_{\tilde{u}_j} = 200$, 210 , and $220\,GeV$ from top to bottom, respectively. The cross section is largest for λ'_{1j1} due to the incoming valence quark. The other two cross sections are suppressed because of the significantly smaller strange and bottom sea-quark structure functions $s(x)$, $b(x)$, respectively.

In Figure 2, we analogously plot the cross sections $\sigma(e^+ + \bar{u}_j \rightarrow \tilde{\bar{d}}_k \rightarrow e^+ + \bar{u}_j)$ as a function of the couplings λ'_{11k} and λ'_{12k} for the three squark mass values $M_{\tilde{d}_k} = 200$, 210 , and $220\,GeV$. Here, we have included the full R-parity violating width from the two \tilde{d}_j decay modes. These cross sections are both suppressed because of the small up and charm sea-structure functions $\bar{u}(x)$ and $c(x)$, respectively, as well as the increased width.

We now compare the plotted cross sections with the hatched band of Eq.(6), and the bounds in the second row of Table 1. We obtain the following set of solutions where R-parity

violation can explain the excess in the HERA data.

$$\begin{aligned}
(1) \quad \lambda'_{121} &\approx 0.015, & \tilde{c}, \quad M_{\tilde{c}} &= (210 \pm 20) \text{ GeV} \\
(2) \quad \lambda'_{131} &\approx 0.015, & \tilde{t}, \quad M_{\tilde{t}} &= (210 \pm 20) \text{ GeV} \\
(3) \quad \lambda'_{112} &\approx 0.1^*, & \tilde{u}, \quad M_{\tilde{u}} &< 210 \text{ GeV} \\
(4) \quad \lambda'_{122} &\approx 0.085^*, & \tilde{c}, \quad M_{\tilde{c}} &< 205 \text{ GeV} \\
(5) \quad [\lambda'_{113} &\approx 0.12^*, & \tilde{u}, \quad M_{\tilde{u}} &\approx 190 \text{ GeV}] \\
(6) \quad \lambda'_{112} &\approx 0.1^*, & \tilde{s}, \quad M_{\tilde{s}} &< 205 \text{ GeV} \\
(7) \quad \lambda'_{113} &\approx 0.1^*, & \tilde{b}, \quad M_{\tilde{b}} &< 205 \text{ GeV} \\
(8) \quad [\lambda'_{121} &\approx 0.12^*, & \tilde{d}, \quad M_{\tilde{d}} &\approx 190 \text{ GeV}]
\end{aligned} \tag{11}$$

In each row we first present the approximate value of the required Yukawa coupling, then denote the produced squark and the mass range of the squark which is viable. The coupling values denoted by the star (*) are on the limiting value of the bounds given in Table 1. The solutions (11.5) and (11.8) are borderline with respect to the mass and we have only included them because of the uncertainty in the data. Thus we obtain many solutions; however, the preferred solutions which are well within the constraints are (11.1) and (11.2) with a produced scalar charm quark and a scalar top quark (“stop”), respectively. Before discussing the other squark decay modes, we note that within supersymmetric unification scenarios there is a possibility for a very light stop, possibly even the LSP [29]. The corresponding scenario at HERA has been discussed in great detail by Kon *et al.* [17]. For a stop-LSP, the process (2) would be the only decay. We shall show below that this solution is almost excluded by the *D*0 leptoquark search data.

There is one possible further solution, which is intriguing. Combining the solutions (11.3) and (11.6), it is possible that HERA has produced two different squarks. One would expect the required coupling to be reduced by about a factor $\sqrt{2}$ to $\lambda'_{112} = 0.07$ which is well away from the indirect bound. We have rerun our cross section program and have confirmed this estimate to obtain the solutions

$$\lambda'_{112} = 0.07, \quad \tilde{u} \& \tilde{s}, \quad M_{\tilde{q}} = 200 \text{ GeV}, \tag{12}$$

$$\lambda'_{112} = 0.1, \quad \tilde{u} \& \tilde{s}, \quad M_{\tilde{q}} = 210 \text{ GeV}. \tag{13}$$

The first solution has some lee-way in the coupling.

4.2 Gaugino Decays of the Squark

In this Subsection we wish to discuss the case where the produced squark is not the LSP and can thus have further supersymmetric decay modes. (This section has no analogy for leptoquarks.) As noted above, supersymmetry dramatically extends the spectrum of the SM. It is way beyond the scope of this paper to perform a systematic study of all the possible decay chains. Instead, we focus on two specific cases which are well motivated by the renormalisation group studies of the MSSM [30]. (a) The lightest neutralino, $\tilde{\chi}_1^0$, is

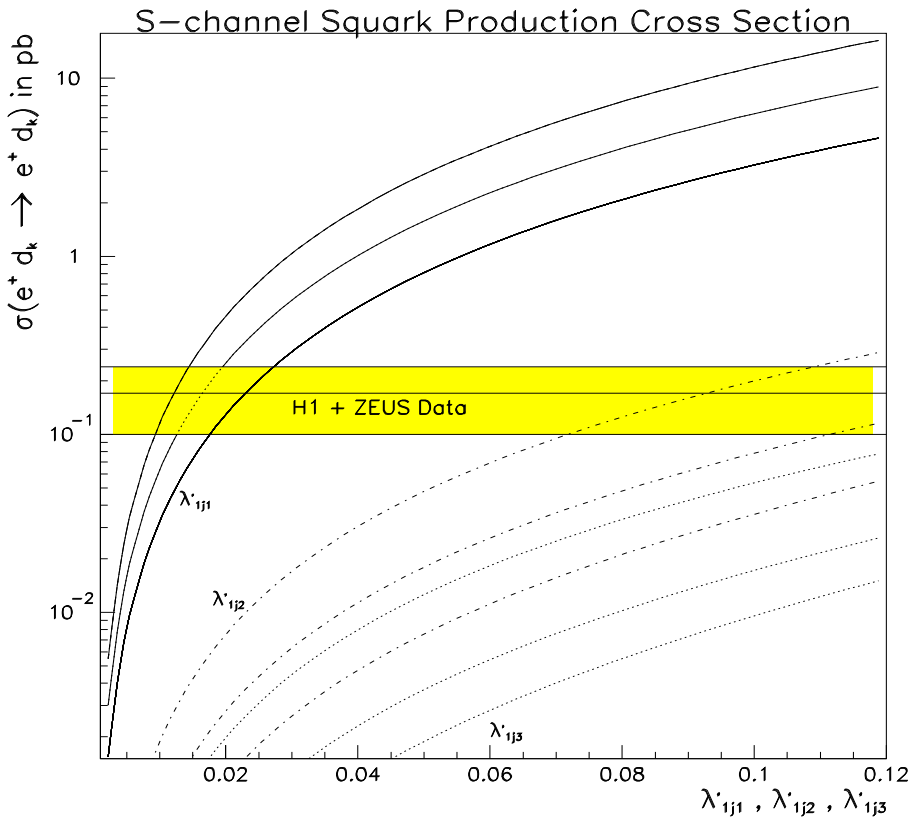


Figure 1: Excess cross-section $\sigma(e^+ d_k \rightarrow e^+ d_k)$ for a s-channel \tilde{u}_j -squark resonance (including the DIS interference term) for $Q^2 > 20,000 \text{ GeV}$ as a function of the coupling λ'_{1jk} for the three values of $M_{\tilde{u}_j} = 200, 210, 220 \text{ GeV}$ (top to bottom). The solid lines show the cross-sections for a non-zero coupling λ'_{1j1} (*i.e.* the d valence quark contribution), while the dashed-dotted and dotted lines show the cross-sections for the non-zero couplings λ'_{1j2} , and λ'_{1j3} (*i.e.* the *s*, and *b* sea quark contributions), respectively. Here, we assume that the only allowed squark decay mode is $\tilde{u}_j \rightarrow e^+ + d_k$. The hatched region shows the high Q^2 excess cross-section $\sigma_{ex} = (0.17 \pm 0.07) \text{ pb}$.

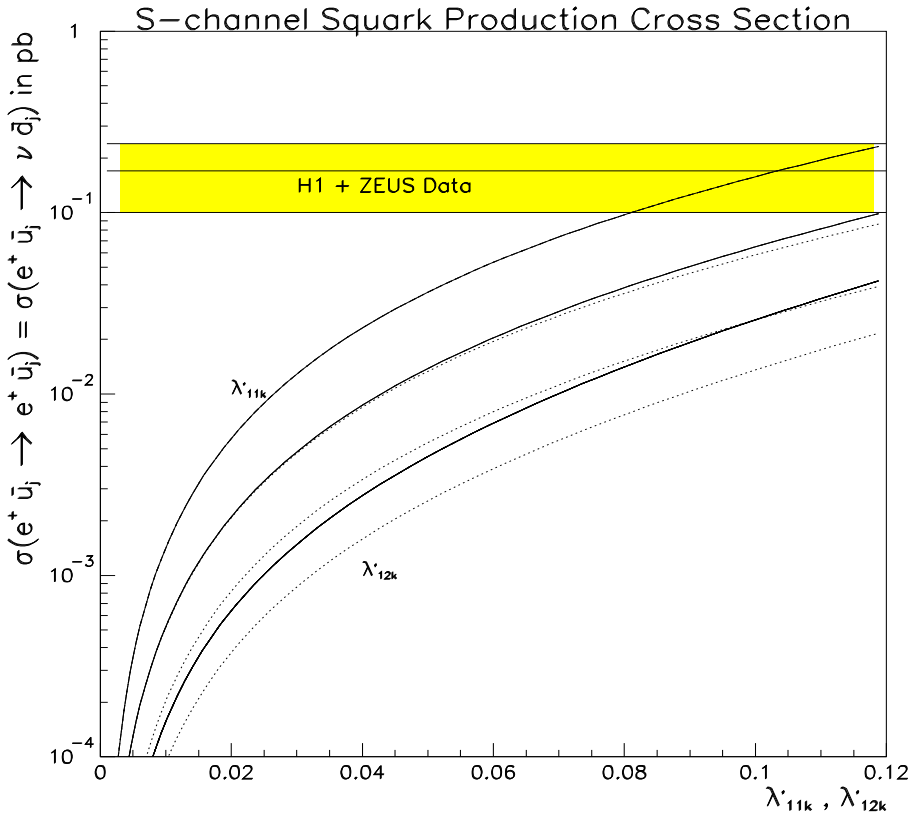


Figure 2: Excess cross-section $\sigma(e^+\bar{u}_j \rightarrow e^+\bar{u}_j) = \sigma(e^+\bar{u}_j \rightarrow \nu\bar{d}_j)$ for a s-channel \tilde{d}_k -squark resonance (including the DIS interference term) for $Q^2 > 20,000 \text{ GeV}$ as a function of the coupling λ'_{1jk} for the three values of $M_{\tilde{d}_k} = 200, 210, 220 \text{ GeV}$ (top to bottom). The solid lines show the cross-sections for a non-zero coupling λ'_{11k} (*i.e.* the u -bar sea quark contribution), while the dotted lines show the cross-sections for the non-zero coupling λ'_{12k} (*i.e.* the c -bar sea quark contributions), respectively. Here, we assume that the only allowed squark decay modes are $\tilde{d}_k \rightarrow e^+ + \bar{u}_j$ and $\tilde{d}_k \rightarrow \bar{\nu} + \bar{d}_j$. The hatched region shows the high Q^2 excess cross-section $\sigma_{ex} = (0.17 \pm 0.07) \text{ pb}$.

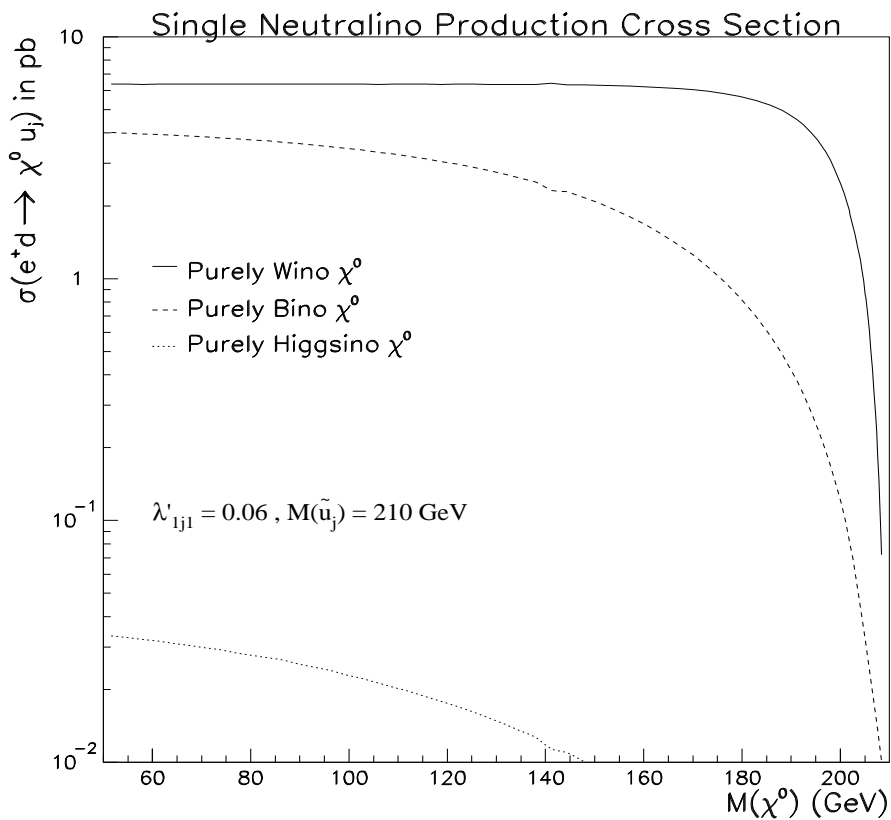


Figure 3: Cross-section $\sigma(e^+d \rightarrow \chi^0 u_j)$ for single neutralino production at HERA for the coupling $\lambda'_{1j1} = 0.06$ and $M_{\tilde{u}_j} = 210 \text{ GeV}$ as a function of the neutralino mass. The solid, dashed and dotted lines show the cross-sections for a neutralino which couples purely Wino-, Bino-, or Higgsino-like, respectively.

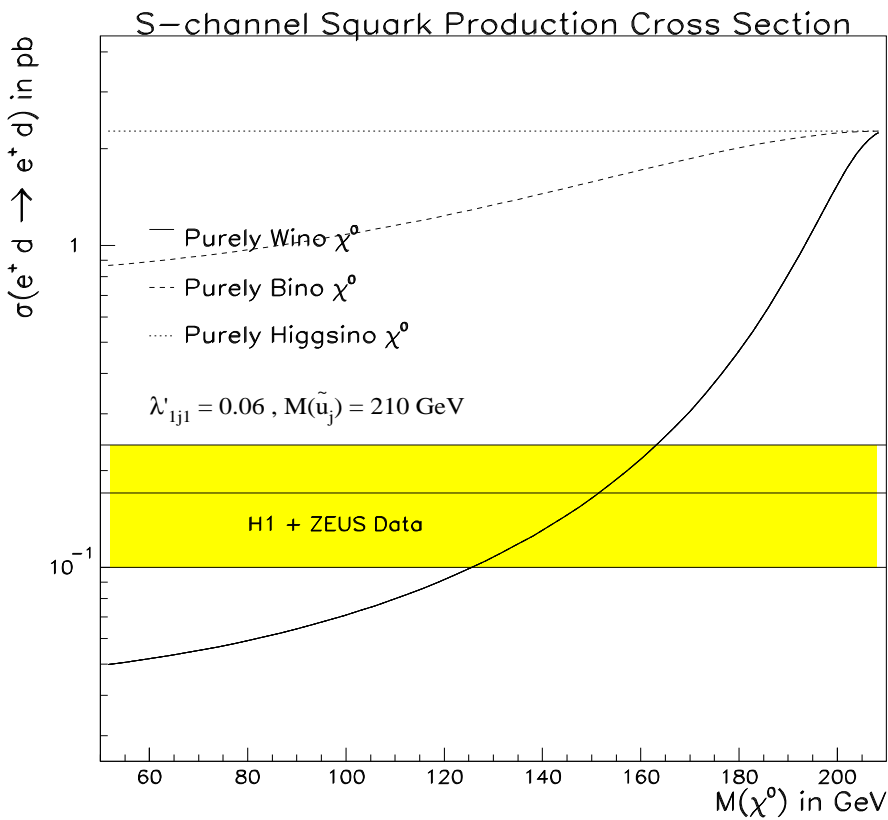


Figure 4: Effect of the additional decay mode $\tilde{u}_j \rightarrow \chi^0 u_j$ on the excess cross-section $\sigma_{ex}(e^+ d \rightarrow e^+ d)$ for a s-channel \tilde{u}_j -squark resonance (including the DIS interference term) for $Q^2 > 20,000 \text{ GeV}$, $\lambda'_{1j1} = 0.06$ and $M_{\tilde{u}_j} = 210 \text{ GeV}$, as a function of the neutralino mass. The hatched region shows the high Q^2 excess cross-section $\sigma_{ex} = (0.17 \pm 0.07) \text{ pb}$.

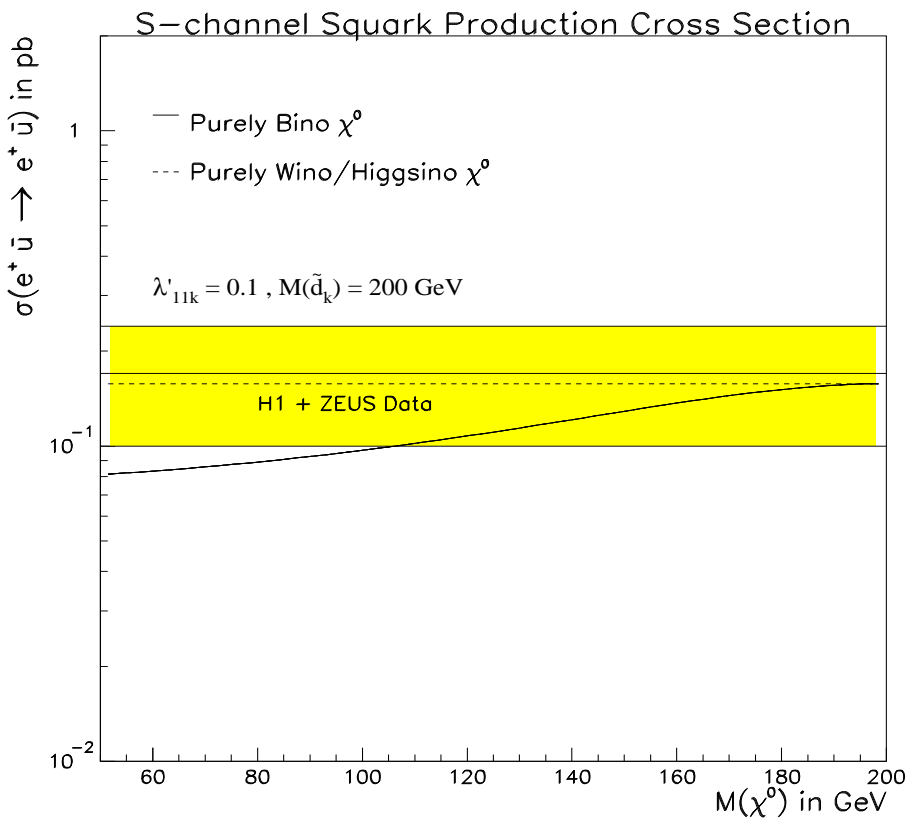


Figure 5: Effect of the additional decay mode $\tilde{d}_k \rightarrow \chi^0 \bar{d}_k$ on the excess cross-section $\sigma(e^+\bar{u} \rightarrow e^+\bar{u})$ for a s-channel \tilde{d} -squark resonance (including the DIS interference term) for $Q^2 > 20,000 \text{ GeV}$, $\lambda'_{11k} = 0.1$ and $M_{\tilde{d}_k} = 200 \text{ GeV}$ as a function of the neutralino mass. The hatched region shows the high Q^2 excess cross-section $\sigma_{ex} = (0.17 \pm 0.07) \text{ pb}$.

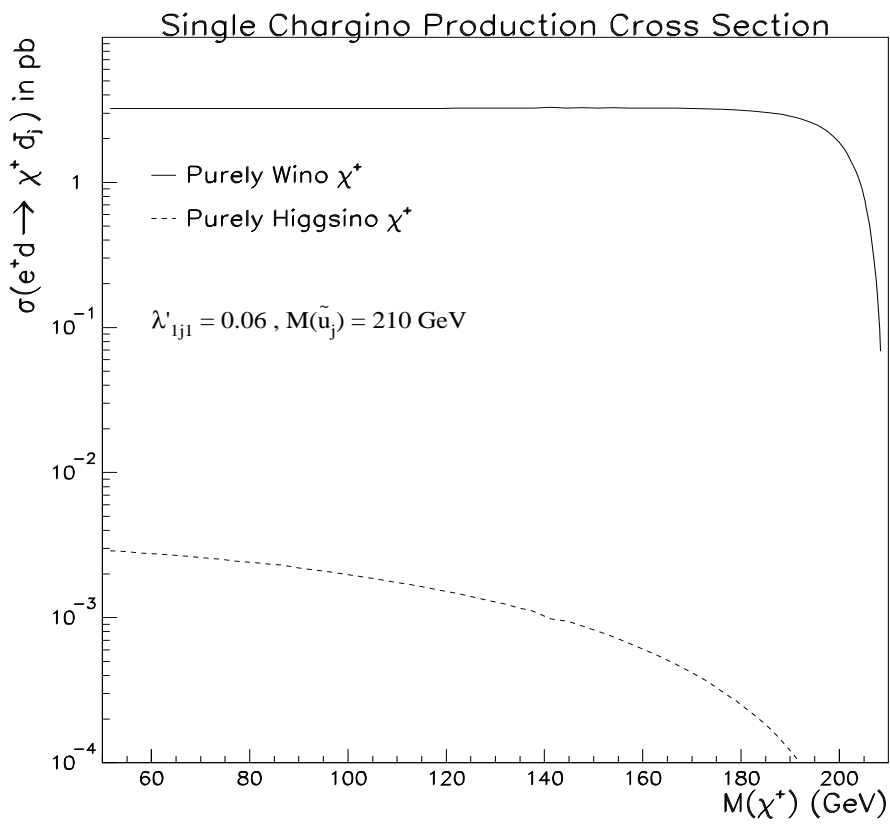


Figure 6: Cross-section $\sigma(e^+d \rightarrow \chi^+ d_j)$ for single chargino production at HERA for the coupling $\lambda'_{1j1} = 0.06$ and $M_{\tilde{u}_j} = 210 \text{ GeV}$ as a function of the chargino mass. The solid and dashed lines show the cross-sections for a chargino which couples purely Wino-, or Higgsino-like, respectively.

lighter than the produced squark, $M_{\tilde{\chi}_1^0} < M_{\tilde{u}_j}$, $M_{\tilde{d}_k}$ and (b) The lightest chargino, $\tilde{\chi}_1^+$, is lighter than the produced squark, $M_{\tilde{\chi}_1^+} < M_{\tilde{u}_j}$, $M_{\tilde{d}_k}$.

(a) If

$$M_{\tilde{\chi}_1^0} < M_{\tilde{u}_j}, M_{\tilde{d}_k}, \quad (14)$$

then we have the following additional interactions at HERA³

$$e^+ + \bar{u}_j \rightarrow \tilde{d}_k \rightarrow \tilde{\chi}_1^0 + \bar{d}_k, \quad (15)$$

$$e^+ + d_k \rightarrow \tilde{u}_j \rightarrow \tilde{\chi}_1^0 + u_j. \quad (16)$$

The production cross section depends on the admixture of the neutralino mass eigenstate. A systematic study is beyond the scope of this paper. In order to determine the cross section we focus on three special limiting cases: a purely Wino-, a purely Bino- and a purely Higgsino- $\tilde{\chi}_1^0$. In Figure 3 we plot the production cross section $\sigma(e^+ + d_k \rightarrow \tilde{\chi}_1^0 + u_j)$ as a function of the neutralino mass for these 3 special cases. We have fixed the squark mass at 210 GeV and the Yukawa coupling $\lambda'_{1j1} = 0.06$. For a purely Higgsino-neutralino, the production cross section is small ($< 3 \cdot 10^{-2}\text{ pb}$) and is not observable at HERA. For a gaugino-neutralino, the cross section is several pb for masses as large as 180 GeV . With the present luminosity, HERA could possibly have already produced several tens of neutralinos, upto about 100 per experiment. The neutralino decay modes are [16]

$$\tilde{\chi}_1^0 \rightarrow \{e^- u_j \bar{d}_k, e^+ \bar{u}_j d_k, \nu_e d_j \bar{d}_k, \bar{\nu}_e \bar{d}_j d_k\}. \quad (17)$$

The branching fractions also depend on the admixture of the neutralino. The most visible decay for a positron beam is $\tilde{\chi}_1^0 \rightarrow e^- u_j \bar{d}_k$, *i.e.* to the final state electron [8]. This requires charge identification of high p_T electrons and can be searched for in the present and upcoming data.

By including the neutralino decay of the squark we have increased the total decay width of the squark. This in turn reduces the resonant production cross sections plotted in Figure 1. In Figure 4, we show this effect for the three neutralino admixtures and for $\lambda'_{1j1} = 0.06$, $M(\tilde{u}_j) = 210\text{ GeV}$. The change in the leptoquark-like cross section (squark LSP) is negligible for the Higgsino-neutralino. For a Bino-neutralino, the cross section can drop by about a factor 2. For a Wino-neutralino the production cross section can drop by more than an order of magnitude.

If we include a Bino- or Wino- $\tilde{\chi}_1^0$ we must reconsider the solutions presented in Section 4.1. For the same coupling λ'_{1jk} , the rate for (8,10) will go down when including the neutralino. This can be compensated by increasing the Yukawa coupling, if allowed. For solution (11.2), the coupling is well below the indirect bound of Table 1. For example, if we raise $\lambda'_{121} = 0.015$ by a factor of 4 to $\lambda'_{121} = 0.06$, we obtain a new solution for a purely Wino- $\tilde{\chi}_1^0$ with mass $M_{\tilde{\chi}_1^0} = 130 - 160\text{ GeV}$, as can be seen in Figure 4. For a coupling $\lambda'_{121} \approx 0.025$ we can also obtain a new solution for a purely Bino- $\tilde{\chi}_1^0$.

³There are further diagrams but the resonant diagram dominates. In the second process, the case $j = 3$ is suppressed by the large top-quark mass and we do not further consider it.

We can similarly consider the effects of the decay $\tilde{d}_k \rightarrow \tilde{\chi}_1^0 + \bar{d}_k$ on the production cross section $\sigma(e^+ \bar{u}_j \rightarrow e^+ \bar{u}_j)$. This is shown in Figure 5. Since the produced squark is an $SU(2)$ singlet, the effect is small for the Wino- $\tilde{\chi}_1^0$ as well as the Higgsino- $\tilde{\chi}_1^0$. For a Bino- $\tilde{\chi}_1^0$, the production rate can be reduced by about a factor of 2. However, there is little room within the coupling constant in this case.

(b) We can repeat the analogous analysis for a chargino with

$$M_{\tilde{\chi}_1^+} < M_{\tilde{u}_j}, M_{\tilde{d}_k}, \quad (18)$$

in which case we obtain the additional interactions

$$e^+ + \bar{u}_j \rightarrow \tilde{d}_k \rightarrow \tilde{\chi}_1^+ + \bar{u}_k, \quad (19)$$

$$e^+ + d_k \rightarrow \tilde{u}_j \rightarrow \tilde{\chi}_1^+ + d_j. \quad (20)$$

We consider the two limiting cases, where the chargino is pure Wino- $\tilde{\chi}_1^+$ or pure Bino- $\tilde{\chi}_1^+$. In Figure 6 we plot the single chargino production cross section $\sigma(e^+ d_k \rightarrow \tilde{\chi}_1^+ \bar{d}_j)$ for these two cases for $\lambda'_{1j1} = 0.06$, and $M(\tilde{u}_j) = 210 \text{ GeV}$. For the pure Higgsino case, the cross section is highly suppressed. These decays can be neglected. For the purely Wino case the cross section is $\approx 3 \text{ pb}$ for $M(\tilde{\chi}_1^+) < 190 \text{ GeV}$. The chargino decays to

$$\tilde{\chi}_1^+ \rightarrow \{\nu_e u_j \bar{d}_k, \bar{\nu}_e \bar{u}_j d_k, e^- d_j \bar{d}_k, e^+ \bar{d}_j d_k\}. \quad (21)$$

Again, the best search mode for a positron beam is the final state electron decay which can be detected at HERA. The chargino production will affect the leptoquark like production analogously to the Bino- and Wino-neutralino cases. Again, this leads to new solutions.

Summarizing, the solutions (11.1) and (11.2) as well as the special solution (12) can allow for substantial decays to gauginos. The other solutions can only allow for Higgsino-like gauginos to be lighter since the decay rates are negligible. Note that the new processes via gaugino decays would be reconstructed at random x and Q^2 for both NC and CC.

5 Tests at HERA

There are several tests of the R-parity violating hypothesis which can be performed at HERA.

1. If HERA is switched back to $e^- p$ collisions the processes (8) -(10) would change to their charge conjugates

$$e^- + u_j \rightarrow \tilde{d}_k \rightarrow e^- + u_j, \quad (22)$$

$$e^- + u_j \rightarrow \tilde{d}_k \rightarrow \nu_e + d_j, \quad (23)$$

$$e^- + \bar{d}_k \rightarrow \tilde{u}_j \rightarrow e^- + \bar{d}_k. \quad (24)$$

For $k = 1$ or $j = 1$ the event rates would increase or decrease, respectively by

$$\begin{aligned} u(x, Q^2)/\bar{u}(x, Q^2) &\approx 6.5, & \text{for } x = 0.45, Q^2 = 4 \cdot 10^4 \text{ GeV}^2, \\ \bar{d}(x, Q^2)/d(x, Q^2) &\approx 0.37, \end{aligned} \quad (25)$$

where we have used the GRV94 structure functions [31]. These changes are readily observable, once an effect has been established for a positron beam. For the other solutions with higher generation incoming quarks, there is no difference between the $q(x, Q^2)$ distribution and the $\bar{q}(x, Q^2)$ distribution and we expect no effect.

2. In the operator $L_1 Q_j \bar{D}_k$, L_1 refers to the first generation lepton $SU(2)$ *doublet* superfield. Therefore, the positron in (8)-(10) is *right*-handed, and the electron in (22)-(24) is *left*-handed. Thus, when the electron/positron polarisers are installed the event rate should double or vanish depending on which polarisation is chosen for the lepton beam [6]. This effect is independent of the quark generation indices.
3. Within supersymmetry with broken R-parity, the nature of the lightest supersymmetric particle (LSP) is unknown. The decay spectrum of the produced squarks depends on the supersymmetry spectrum as a whole. In the previous Section, we considered the case where a neutralino or chargino is lighter than the squark. This leads to an additional electron (positron) signal for a positron (electron) beam, which can be searched for.

The most important conclusion from this is that HERA itself can determine the nature of the observed effect. The second conclusion we draw is that it is essential for HERA to first continue running in the present mode and *not* switch to an electron beam or run at lower energy. This way both experiments can establish whether there is a genuine effect or whether it is merely a statistical fluctuation. If HERA did switch to an electron beam and the effect is due to the production of up-like squarks the excess would be decreased and require longer running time to establish its nature. We could then end up in one year with two separate non-significant excesses and being no-more the wiser.

6 Signals at LEP 2

In this Section we discuss three tests of the R-parity violation hypothesis at LEP 2. (1) Pair production of selectrons. The pair production of squarks at LEP 2 with $m_{\tilde{q}} = 200\,GeV$ is kinematically prohibited. Selectrons on the other hand, could be kinematically accessible at LEP without having been seen at HERA. In particular, they can decay through the same R-parity violating operator $L_1 Q_j \bar{D}_k$. With the present data samples of $L \sim 25\,pb^{-1}$ per experiment at $\sqrt{s} = 130 - 172\,GeV$, selectron masses $m_{\tilde{e}} < 70\,GeV$ are accessible [32]. (2) Gauginos, if light, can be pair produced and subsequently can decay via $L_1 Q_j \bar{D}_k$ to visible leptonic final states. (3) Virtual t-channel exchange of squarks would give a contribution to the SM process $e^+ e^- \rightarrow q\bar{q}$ [33, 34]. We investigate these three effects in the following.

6.1 Selectron pair production and the ALEPH 4-jet Anomaly

If the selectrons are lighter than the neutralinos, the dominant decay channel for the Yukawa coupling size of interest is:

$$\tilde{e}_{L,R} \rightarrow u_j \bar{d}_k. \quad (26)$$

Selectron pair production would then give rise to 4-jet signals at LEP 2 through the process $\tilde{e}_L \tilde{e}_R \rightarrow (u_j \bar{d}_k)(\bar{u}_j d_k)$. This scenario has been investigated in [35], where it was found that selectron masses of $m_{\tilde{e}_L} = 58 \text{ GeV}$, $m_{\tilde{e}_R} = 48 \text{ GeV}$ could explain the anomalous invariant mass peak of 4-jet final states observed by ALEPH [36], as well as the apparent difference in mass $\Delta M \sim 10 \text{ GeV}$. It must be pointed out that the ALEPH anomaly is not seen by the other three LEP experiments, and its origin is at present not understood. In this Subsection, we will assume that the ALEPH effect is due to new physics. It is then intriguing to ask whether the HERA excess when interpreted as s-channel squark production is compatible with the above interpretation of the ALEPH 4-jet signal. In order to explain the ALEPH data there are several requirements on λ'_{1jk} [35].

- (a) The solution to the ALEPH 4-jet anomaly requires the associated production of an $SU(2)$ singlet selectron (\tilde{e}_R) and an $SU(2)$ doublet selectron (\tilde{e}_L) with different mass. The \tilde{e}_R can not decay directly via the operator $L_1 Q_j \bar{D}_k$, only via the mixing with the \tilde{e}_L . If this mixing is small [35] then for small λ' the \tilde{e}_R will be long-lived. This in turn can be observed in the ALEPH detector but wasn't. Thus the coupling must be large: $\lambda'_{1jk} > 0.01$ [35].
- (b) The ALEPH 4-jet data excludes final states which contain b-quarks, and favours u,d,s quark final states; charm quarks are disfavoured, but not excluded. Including the tight constraints on λ'_{111} one arrives at three solutions: λ'_{112} , λ'_{121} , λ'_{122} (*c.f.* Table 2). The solution with $\lambda'_{112} \gtrsim 0.01$ is favoured by the ALEPH data [35].

Coupling	Process which can explain the ALEPH 4-jet anomaly
$\lambda'_{112} \gtrsim 0.01$	$\tilde{e}_L \tilde{e}_R \rightarrow u \bar{u} s \bar{s}$
$\lambda'_{121} > 0.01$	$\tilde{e}_L \tilde{e}_R \rightarrow c \bar{c} d \bar{d}$
$\lambda'_{122} > 0.01$	$\tilde{e}_L \tilde{e}_R \rightarrow c \bar{c} s \bar{s}$

Table 2: Allowed couplings which can explain the ALEPH 4-jets.

As discussed in Section 4, the HERA high Q^2 excess, too, can be explained by these three couplings (*c.f.* Table 3).

We now consider these three solutions when combining the ALEPH and the HERA data.

(a) $\lambda'_{112} = 0.1$. According to Section 4.2, the branching ratio $\tilde{s} \rightarrow s \chi^0$ must then be small. The HERA excess cross-section can be explained for neutralinos with $M(\tilde{\chi}^0) \gtrsim 100 \text{ GeV}$ (*c.f.* Figure 5). Additionally, one would observe high Q^2 charged current events at a rate $\sigma(e^+ \bar{u} \rightarrow \nu \bar{d}) = 0.16 \text{ pb}$. For this coupling, there is the further solution (11.3). We show below that this is practically excluded by the TEVATRON data.

Coupling	Process explaining the HERA high Q^2 anomaly	Additional signals at HERA
$\lambda'_{112} = 0.1$	$e^+\bar{u} \rightarrow \tilde{s} \rightarrow e^+\bar{u}$ $e^+\bar{d} \rightarrow \tilde{u} \rightarrow e^+\bar{s}$	$e^+\bar{u} \rightarrow \tilde{s} \rightarrow \nu\bar{d}$ -
$\lambda'_{121} > 0.015$	$e^+\bar{d} \rightarrow \tilde{c} \rightarrow e^+\bar{d}$	$e^+\bar{d} \rightarrow \tilde{c} \rightarrow \chi^0 u$
$\lambda'_{122} = 0.085$	$e^+\bar{s} \rightarrow \tilde{c} \rightarrow e^+\bar{s}$	-

Table 3: Allowed couplings which can explain the HERA high Q^2 anomaly.

(b) $\lambda'_{121} > 0.015$. In order to fit the ALEPH data comfortably, the coupling λ'_{121} should be as large as possible. This evades the effects of lifetime (which are now amplified by the presence of charm in the 4-jet final states). But for a large coupling (say $\lambda'_{121} = 0.06$), the HERA excess cross-section of 0.17 pb only fits the predicted cross-section if the squark coupling to the neutralino is large. The additional decay mode $\tilde{c} \rightarrow \tilde{\chi}^0 c$ must reduce the predicted cross-section $\sigma(e^+\bar{u} \rightarrow \tilde{c} \rightarrow e^+\bar{u})$ from 2.2 pb to 0.17 pb (Figure 4). A neutralino with $M_{\chi^0} = 150\text{ GeV}$ which couples with a dominant bino component indeed fits the data. The additional process $e^+\bar{u} \rightarrow \tilde{c} \rightarrow \tilde{\chi}^0 c$ has a cross-section of 6 pb (Figure 3), which would predict around 200 events between the two experiments *H1* and *ZEUS* in the 1995/1996 data; a signal which is observable⁴. That cross-section decreases, as the value of λ'_{121} is decreased, since the neutralino mass has to be increased correspondingly to fit the data.

(c) $\lambda'_{122} = 0.085$, least favoured by the ALEPH data. No additional signals are expected at HERA. This solution is also practically excluded by the TEVATRON data.

We conclude that the ALEPH anomaly and the HERA excess can in principle be simultaneously explained by two scenarios: $\lambda'_{112} = 0.1, \lambda'_{121} > 0.015$. The most favoured scenario ($\lambda'_{112} = 0.1$) also predicts an excess in high Q^2 charged current events at HERA, while the less favoured scenario ($\lambda'_{121} > 0.015$) predicts events with additional squark decays to gauginos.

6.2 Other Signals at LEP 2

Let us now discuss the constraints placed on the supersymmetric spectrum by the solutions of eq.(11). We find four scenarios which determine the gaugino spectrum:

- (a) Solution (11.1) can accommodate gauginos which are substantially lighter than $M_{\tilde{q}}$ and couple electroweakly to the squarks (e.g. non-Higgsino like).
- (b) Solution (11.2) requires $M_{\tilde{\chi}^0} > M_{\tilde{t}} - M_t$, and $M_{\tilde{\chi}^\pm} > M_{\tilde{t}} - M_b$.
- (c) All other solutions require either large gaugino masses ($\gtrsim 200\text{ GeV}$), which is of no interest to LEP 2, or

⁴Note that currently the upper limit on this process is at $\lambda'_{121} \leq 0.06$ (for $M_{\tilde{\chi}} = 80\text{ GeV}$) from a search for $e^+P \rightarrow \tilde{\chi}^0 + q$ by the *H1* collaboration (1994 data only) [37].

Anti-ISR cut	$\sigma(e^+e^- \rightarrow d\bar{d})$	$\sigma(e^+e^- \rightarrow d\bar{d})$	Effect on total cross-section $\sigma(e^+e^- \rightarrow q\bar{q})$
	SM only	SM plus t-channel \tilde{c} exchange	
$\sqrt{s'/s} > 0.9$	18.62pb	18.82pb	+0.22%
	3.31pb	3.49pb	+0.88%
$\sqrt{s'/s} > 0.9$	$\sigma(e^+e^- \rightarrow u\bar{u})$	$\sigma(e^+e^- \rightarrow u\bar{u})$	
	SM only	SM plus t-channel \tilde{s} exchange	
$\sqrt{s'/s} > 0.9$	18.40pb	18.13pb	-0.29%
	5.30pb	5.08pb	-1.07%

Table 4: Cross-section values for the SM process and the SM plus t-channel squark exchange for $M_{\tilde{q}} = 200\text{ GeV}$ and $\lambda = 0.1$ at $\sqrt{s} = 190\text{ GeV}$.

- (d) they can accommodate light gauginos which a small coupling (e.g. Higgsino-like) to the squarks.

In summary, we conclude that cases (a), (b) and (d) are interesting for LEP 2 since charginos and neutralinos might be discovered up to the kinematic limit of $\sqrt{s}/2$. LEP 2 itself however has no way of testing the R-parity hypothesis of the high Q^2 HERA excess, since the non-observation of R-parity violating SUSY at LEP 2 cannot rule out that the HERA effect is indeed a sign of a s-channel squark resonance.

6.3 Virtual Effects at LEP 2 from t-channel Squark Exchange

The cross-section for this effect can be obtained from the leptoquark calculation of [38] by crossing, and we quote it in the appendix for completeness. This effect has been studied in the literature [33, 34]. The magnitude of the effect is small, since the diagram is proportional to λ'^2 . Figure 7 shows the contribution of t-channel \tilde{c} and \tilde{s} exchange for $M_{\tilde{q}} = 200\text{ GeV}$ at $\sqrt{s} = 190\text{ GeV}$. Note, that the effect due to a \tilde{c} exchange gives a positive contribution to $\sigma(e^+e^- \rightarrow d\bar{d})$, while the \tilde{s} exchange gives a negative contribution to $\sigma(e^+e^- \rightarrow u\bar{u})$.

The overall effect on the total cross-section is shown in Table 4. We have also included a column with cross-sections including an anti-ISR cut $\sqrt{s'/s} > 0.9$, where s is the center of mass energy of the incoming lepton beams, and s' is the center of mass energy of the outgoing $q\bar{q}$ pair. The cut enhances the contribution of the t-channel squark exchange to the total $q\bar{q}$ cross-section. Nevertheless, the total effect is still less than 1.07%, and we therefore conclude that the effect of virtual t-channel squark exchange is too small to be observed at LEP 2 for squark masses of $M_{\tilde{q}} = 200\text{ GeV}$ and couplings of $\lambda' = 0.1$ even for a Luminosity of 400 pb^{-1} (expected to be delivered to the four experiments for the 1997 run).

Very recently, the OPAL collaboration have performed the measurement [39]. For squark masses of 200 GeV , they are only sensitive to couplings $\lambda'_{1jk} > 0.2$.

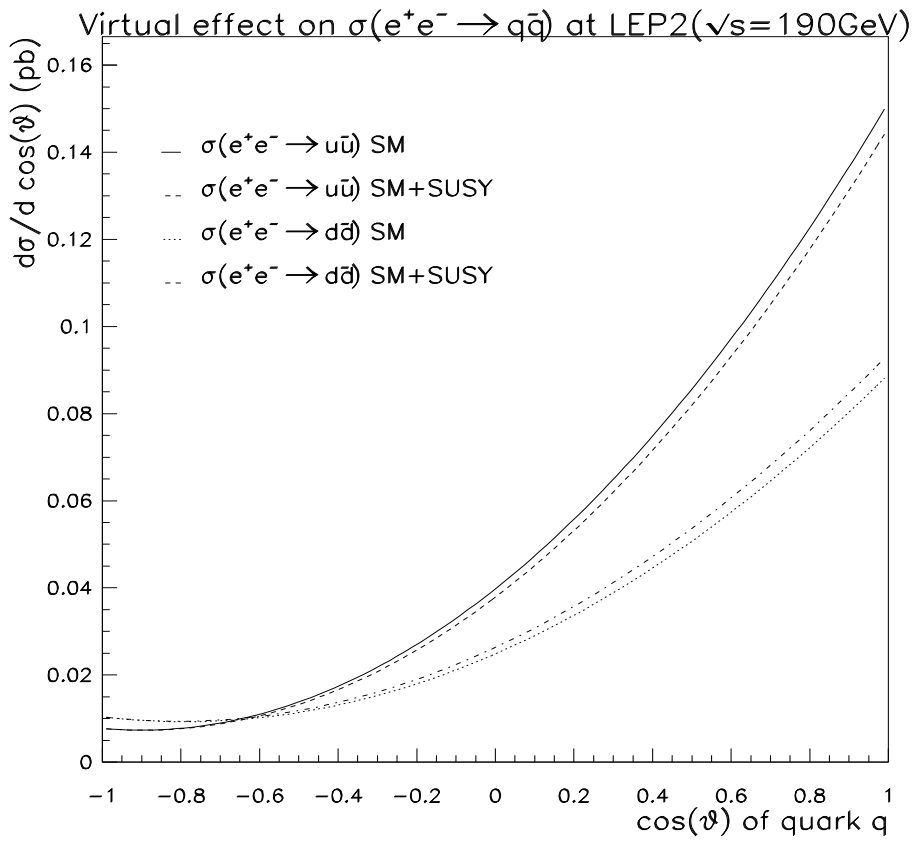


Figure 7: Differential cross-sections $d\sigma/d\cos\theta$ for $M_{\tilde{c}}, M_{\tilde{s}} = 200\text{GeV}$ and $\lambda'_{121}, \lambda'_{112} = 0.1$ respectively. We have included Initial State Radiative corrections, and used the anti-ISR cut $\sqrt{s'/s} > 0.9$ (see text).

7 Signals at the Tevatron

There are several potential tests of the above ‘supersymmetry with broken R-parity’ hypothesis (produce one squark via operator $L_1 Q_j \bar{D}_k$) at the TEVATRON: (a) t -channel squark exchange interfering with Drell-Yan production, (b) single squark production, and (c) squark pair production.

(a) The operators $L_1 Q_j \bar{D}$ can also contribute to Drell-Yan production via the t -channel exchange of a squark. The dominant effect is the interference with the SM. This has been studied in [33]. However, the above study did not consider the for us relevant range at the TEVATRON, basically because it was not feasible with the projected luminosity. We have repeated the analysis for the solutions (1), (2), (6), and (7) which involve incoming first generation quarks. In all cases we found a negligible effect ($< 1\%$) well below the uncertainty of the structure functions. This is not feasible even for the TEVATRON upgrade. For the other solutions the effect is even smaller.

(b) The scalar quarks can be singly produced via the parton-level processes

$$g + u_j \rightarrow e^+ + d_k, \quad (27)$$

$$g + d_k \rightarrow e^- + u_j, \quad (28)$$

as well as the complex conjugate production mechanisms. Here g denotes a parton gluon. This is completely equivalent to single leptoquark production at the TEVATRON which has been analysed in [40]. The production is proportional to λ'_{1jk}^2 . For our solutions (3) - (8) (incoming sea-quark), we have $\lambda'_{1j2}, \lambda'_{11k} \approx 0.1$ and $M_{\tilde{u}_j} \approx 200 \text{ GeV}$. From Fig. 2 Ref.[40] we expect less than 0.5 events for an integrated luminosity of 110 pb^{-1} , which is not detectable. For our other solutions (1) and (2) the rate is significantly lower, since $\lambda'_{1j1} \approx 0.02$. Thus, provided the HERA signal is a true anomaly, we do not expect to see any single squark production via the $L_1 Q \bar{D}$ operators at the TEVATRON, even with the upgrade. This conclusion is independent of the supersymmetric spectrum.

(c) Squarks can be pair produced at the TEVATRON via⁵

$$g + g \rightarrow \tilde{q} + \tilde{\bar{q}}, \quad (29)$$

$$q + \bar{q} \rightarrow \tilde{q} + \tilde{\bar{q}}. \quad (30)$$

If the squark only decays via the dominant first lepton generation R-parity violating operator $L_1 Q_j \bar{D}_k$ then this is equivalent to first generation leptoquark production and decay. $D0$ have recently updated their analysis and obtained preliminary lower bounds on such a leptoquark [41]

$$D0 : \begin{aligned} M_{LQ} &> 194 \text{ GeV}, \text{ for } BR(\phi_{LQ} \rightarrow e^\pm q) = 1, \\ &M_{LQ} > 143 \text{ GeV}, \text{ for } BR(\phi_{LQ} \rightarrow e^\pm q) = 0.5. \end{aligned} \quad (31)$$

⁵The second process includes t -channel electron exchange via the R-parity violating operator. For the couplings we consider this contribution is negligible.

The first bound applies for a two-body leptonic branching ratio of 1, *i.e.* the only decay mode is $\phi_{LQ} \rightarrow e^\pm + q$. This can immediately be reinterpreted as a lower bound for up-like squarks, provided they can not decay via gauginos or other supersymmetric particles. The second, weaker bound applies to the case where there is a second decay without a charged lepton and which has equal decay width to the charged lepton decay. This can be reinterpreted as a lower bound for d-like squarks, since as shown in Eqs.(8,9) they have two equal decay modes (provided the final state quark masses can be neglected).

Before applying these bounds we note that they only employ the tree-level cross-section for leptoquark pair-production. In our case, for squark pair production, the next-to-leading order calculation has been done. The production cross section is increased by ≈ 2 [42]. If we include this in the $D0$ -plot the more stringent bound increases by about $20\,GeV$ to $215\,GeV$. This should be further strengthened by combining the $D0$ and CDF leptoquark bounds.

For the down-like squarks, which have a decay branching ratio to charged leptons < 0.5 these $D0$ bounds are not relevant and our previous analysis of Section 4 applies. For the up-like squarks with only R-parity violating decays, solutions (11.1)-(11.5), these bounds apply directly and are very severe. This basically excludes solutions (11.3) - (11.5) and marginally allows solutions (11.1), (11.2) and (12) for a squark LSP. As discussed in Section 4.2, for solution (11.2) we can include further decays to a neutralino or chargino. These will reduce the branching ratio for the two body-decay to a charged lepton and thus reduce the effective $D0$ bound. For the solution with $\lambda'_{121} = 0.06$ involving gaugino decays and discussed in Section 4.2, the branching ratio is reduced well below 0.5 for the Wino-neutralino and to about 0.5 for the Bino-neutralino. This sufficiently reduces the $D0$ bound to make this solution viable.

For the solutions (12,13) where two distinct squarks are produced, we can raise the coupling by a factor $\sqrt{2}$. This increases the production rate by about a factor of two. We then have to include neutralino decay to reduce this by about a factor of two, in order to agree with the HERA data. This corresponds roughly to reducing the 2-body leptonic decay branching ratio by about a factor 2. Thus this model is safe from the $D0$ bound.

We summarise our solutions below.

8 Conclusions

We have discussed the recently observed excess at HERA in the high Q^2 data in the light of supersymmetry with broken R-parity. For a squark LSP, we obtain several solutions, of which most are just barely consistent with the existing bounds, including those from the TEVATRON. When including gaugino decays we obtain the preferred solution $\lambda'_{121} > 0.015$. We have summarised the tests that can be performed at other colliders. We have also considered the simultaneous solution of the ALEPH four-jet anomaly. Our solutions can be summarised as

1. Solution (11.1), with $\lambda'_{121} > 0.015$. Production of \tilde{c} squark including gaugino decays. This solution is most consistent with all the data. It can also accomodate the ALEPH four-jet anomaly for large couplings.
2. Solutions (11.6)-(11.8), with $\lambda'_{112,113,121} \approx 1 - 1.2$. production of \tilde{s}, \tilde{b} , and \tilde{d} squark respectively. Can allow at most additional Higgsino decays. λ'_{112} is also the preferred solution for the ALEPH four-jet anomaly.
3. Solution (12) with $\lambda'_{112} \approx 0.1$. Two squarks are produced: \tilde{u} and \tilde{s} . Must include gaugino decays to accomodate the TEVATRON data comfortably.
4. Solution (11.2) and solution (11.1) without gaugino decays are marginally allowed. They can be tested once the two experiments combine their data at the TEVATRON.

It is amusing to note that in Ref.[14] a model with an anomaly-free family dependent $U(1)_R$ R -gauge symmetry was constructed which predicted the dominant R-parity violating operators $L_1 Q_1 \bar{D}_2, L_1 Q_2 \bar{D}_1$.

We eagerly await further data to confirm or reject this hypothesis. It might then also be possible to make a statement about CC DIS and contributions from supersymmetry decays.

9 Acknowledgements

We thank Jon Butterworth and Ken Long for discussions of the ZEUS data. We thank Sacha Davidson for discussions on indirect bounds.

10 Appendix

10.1 Single Neutralino Production Cross-section at HERA

The cross-sections for the process $e^- P \rightarrow \tilde{\chi}_1^0 + X$ in the approximation where the neutralino is a pure photino have been previously calculated in [8]. In this Section, we generalise the results to the case of a neutralino (which is an admixture of the photino, wino and higgsino weak eigenstates). The differential cross-section for single neutralino production via the R-parity violating coupling λ'_{1jk} at HERA may then be written as

$$\frac{d\sigma(e^+ P \rightarrow \chi^0 + X)}{dxdQ^2} = \frac{1}{16\pi x^2 s^2} (q_d(x, Q^2) |\mathcal{M}(e^+ d_k \rightarrow \chi^0 u_j)|^2 + \bar{q}_u(x, Q^2) |\mathcal{M}(e^+ \bar{u}_j \rightarrow \chi^0 \bar{d}_k)|^2) \quad (32)$$

where $q_d(x, Q^2)$ and $\bar{q}_u(x, Q^2)$ give the probability of finding a d_k -quark and \bar{u}_j -quark respectively inside the proton; s, x, Q^2 are the center of mass energy, the Bjorken scaling

variable and the momentum transfer squared. The Matrix elements can be obtained from [16] by crossing and are given by (neglecting initial state masses):

$$\begin{aligned}
|\mathcal{M}(e^+ d_k \rightarrow \chi^0 u_j)|^2 &= g^2 \lambda_{1jk}^{\prime 2} \{ \\
&\quad \frac{\hat{s}}{(\hat{s} - m_{\tilde{u}j}^2)^2 + \Gamma_{\tilde{u}j}^2 m_{\tilde{u}j}^2} [(a(u_j)^2 + b(u)^2)(\hat{s} - m_{\chi^0}^2 - m_{uj}^2) \\
&\quad + 4a(u_j)b(u)m_{uj}m_{\chi^0}] \\
&\quad + \frac{m_{uj}^2 - u}{(u - m_{\tilde{d}k}^2)^2} [b(\bar{d})^2(m_{\chi^0}^2 - u)] \\
&\quad + \frac{m_{uj}^2 - u}{(t - m_{\tilde{e}}^2)^2} [b(e)^2(m_{\chi^0}^2 - t)] \\
&\quad - \frac{\hat{s} - m_{\tilde{u}j}^2}{[(\hat{s} - m_{\tilde{u}j}^2)^2 + \Gamma_{\tilde{u}j}^2 m_{\tilde{u}j}^2][t - m_{\tilde{e}}^2]} [2a(u_j)b(e)m_{uj}m_{\chi^0}\hat{s} \\
&\quad + b(e)b(u)(\hat{s}^2 + t^2 - u^2 + (m_{\chi^0}^2 + m_{uj}^2)(u - \hat{s} - t))] \\
&\quad + \frac{1}{(t - m_{\tilde{e}}^2)(u - m_{\tilde{d}k}^2)} [b(e)b(\bar{d}) \\
&\quad (t^2 + u^2 - \hat{s}^2 + (m_{\chi^0}^2 + m_{uj}^2)(\hat{s} - t - u) + 2m_{uj}^2 m_{\chi^0}^2)] \\
&\quad + \frac{\hat{s} - m_{\tilde{u}j}^2}{[(\hat{s} - m_{\tilde{u}j}^2)^2 + \Gamma_{\tilde{u}j}^2 m_{\tilde{u}j}^2][u - m_{\tilde{d}k}^2]} [2a(u_j)b(\bar{d})m_{uj}m_{\chi^0}\hat{s} \\
&\quad + b(u)b(\bar{d})(\hat{s}^2 + u^2 - t^2 + (m_{\chi^0}^2 + m_{uj}^2)(t - \hat{s} - u))] \} \quad (33)
\end{aligned}$$

where \hat{s}, t, u are the Mandelstamm variables defined as $\hat{s} = (p_e + p_{dk})^2 = xs, t = (p_e - p_{\chi^0})^2 = -Q^2, u = m_{\chi^0}^2 + m_{dk}^2 - \hat{s} - t$; $g = \frac{e}{\sin \theta_w}$; m_{χ^0}, m_{uj} are the masses of the final state particles, and $m_{\tilde{e}}, m_{\tilde{u}j}, m_{\tilde{d}k}$ are the masses of the exchanged scalar SUSY particles; $\Gamma_{\tilde{u}j}$ is the total width of the scalar $\tilde{u}j$.

$$\begin{aligned}
|\mathcal{M}(e^+ \bar{u}_j \rightarrow \chi^0 \bar{d}_k)|^2 &= g^2 \lambda_{1jk}^{\prime 2} \{ \\
&\quad \frac{m_{dk}^2 - u}{(u - m_{\tilde{u}j}^2)^2} b(u)^2(m_{\chi^0}^2 - u) \\
&\quad + \frac{\hat{s}}{(\hat{s} - m_{dk}^2)^2 + \Gamma_{\tilde{d}k}^2 m_{dk}^2} [(a(d_k)^2 + b(\bar{d})^2)(\hat{s} - m_{\chi^0}^2 - m_{dk}^2) \\
&\quad - 4a(d_k)b(\bar{d})m_{dk}m_{\chi^0}] \\
&\quad + \frac{m_d^2 - t}{(t - m_{\tilde{e}}^2)^2} b(e)^2(m_{\chi^0}^2 - t) \\
&\quad - \frac{1}{(t - m_{\tilde{e}}^2)(u - m_u^2)} b(e)b(u)[t^2 - s^2 + u^2 + (m_{\chi^0}^2 + m_{dk}^2)(s - t - u) + 2m_{dk}^2 m_{\chi^0}^2] \\
&\quad - \frac{\hat{s} - m_{\tilde{d}k}^2}{[(\hat{s} - m_{\tilde{d}k}^2)^2 + \Gamma_{\tilde{d}k}^2 m_{\tilde{d}k}^2][u - m_{\tilde{u}j}^2]} [2a(d_k)b(u)m_{dk}m_{\chi^0}\hat{s} \\
&\quad - b(u)b(\bar{d})(u^2 + s^2 - t^2 + (m_{\chi^0}^2 + m_{dk}^2)(t - s - u))] \\
&\quad - \frac{\hat{s} - m_{\tilde{d}k}^2}{[(\hat{s} - m_{\tilde{d}k}^2)^2 + \Gamma_{\tilde{d}k}^2 m_{\tilde{d}k}^2][t - m_{\tilde{d}}^2]} [2a(d_k)b(e)m_{dk}m_{\chi^0}\hat{s} \\
&\quad - b(e)b(\bar{d})(s^2 + t^2 - u^2 + (m_{\chi^0}^2 + m_{dk}^2)(u - t - s))] \} \quad (34)
\end{aligned}$$

where \hat{s}, t, u are now defined as $\hat{s} = (p_e + p_{uj})^2 = xs$, $t = (p_e - p_{\chi^0})^2 = -Q^2$, $u = m_{\chi^0}^2 + m_{uj}^2 - \hat{s} - t$. The total cross-section can be obtained from eq.(32) by integrating over the x, Q^2 range

$$\begin{aligned} x_{min} &= (m_{\chi^0}^2 + m_{fs}^2)/s \\ x_{max} &= 1 \\ Q_{min}^2 &= \hat{s} - m_{\chi^0}^2 \\ Q_{max}^2 &= s \end{aligned} \quad (35)$$

and m_{fs} is the mass of the final state quark, i.e. m_{uj} , m_{dk} for Eqns. (33),(34) respectively. The coupling constants a,b are given in Table A.1 of reference [16]. The cross-section for the process $e^- P \rightarrow \chi^0 + X$ can be obtained from the above result by charge conjugation:

$$\frac{d\sigma(e^- P \rightarrow \chi^0 + X)}{dxdQ^2} = \frac{1}{16\pi x^2 s^2} (-\bar{q}_d(x, Q^2) |\mathcal{M}(e^- \bar{d}_k \rightarrow \chi^0 \bar{u}_j)|^2 + q_u(x, Q^2) |\mathcal{M}(e^- u_j \rightarrow \chi^0 d_k)|^2) \quad (36)$$

where $|\mathcal{M}(e^- \bar{d}_k \rightarrow \chi^0 \bar{u}_j)|^2 = |\mathcal{M}(e^+ d_k \rightarrow \chi^0 u_j)|^2$ and $|\mathcal{M}(e^- u_j \rightarrow \chi^0 d_k)|^2 = |\mathcal{M}(e^+ \bar{u}_j \rightarrow \chi^0 \bar{d}_k)|^2$.

10.2 Single Chargino Production Cross-section at HERA

The differential cross-section for single chargino production via the R-parity violating coupling λ'_{1jk} at HERA may be written as

$$\frac{d\sigma(e^+ P \rightarrow \chi^+ + X)}{dxdQ^2} = \frac{1}{16\pi x^2 s^2} (-q_d(x, Q^2) |\mathcal{M}(e^+ d_k \rightarrow \chi^+ d_j)|^2 + \bar{q}_u(x, Q^2) |\mathcal{M}(e^+ \bar{u}_j \rightarrow \chi^+ \bar{u}_k)|^2) \quad (37)$$

where the Matrix elements can be obtained from [43] by crossing and are given by

$$\begin{aligned} |\mathcal{M}(e^+ d_k \rightarrow \chi^+ d_j)|^2 &= \frac{g^2 \lambda'_{1jk}^2}{4} \{ \\ &\quad \frac{m_{d_j}^2 - t}{(t - m_{\tilde{\nu}}^2)^2} (\gamma_L^2 + \gamma_R^2) (m_{\chi^+}^2 - t) \\ &+ \frac{\hat{s}}{(\hat{s}^2 - m_{\tilde{u}_j}^2)^2 + \Gamma_{\tilde{u}_j}^2 m_{\tilde{u}_j}^2} [(\delta_L^2 + \delta_R^2) (\hat{s} - m_{\chi^+}^2 - m_{d_j}^2) + 8\mathcal{R}e\{\delta_L \delta_R^* m_{d_j} m_{\chi^+}\}] \\ &- \frac{\hat{s} - m_{\tilde{u}_j}^2}{[(\hat{s} - m_{\tilde{u}_j}^2)^2 + \Gamma_{\tilde{u}_j}^2 m_{\tilde{u}_j}^2][t - m_{\tilde{\nu}}^2]} \mathcal{R}e\{\gamma_L \delta_L^* [\hat{s}^2 + t^2 - u^2 \\ &\quad + (m_{d_j}^2 + m_{\chi^+}^2)(u - s - t)] + 2\gamma_L \delta_R^* m_{d_j} M_{\chi^+} \hat{s}\} \} \end{aligned} \quad (38)$$

where \hat{s}, t, u are defined by $\hat{s} = (p_e + p_{dk})^2 = xs$, $t = (p_e - p_{\chi^+})^2 = -Q^2$, $u = m_{\chi^+}^2 + m_{d_j}^2 - \hat{s} - t$. And

$$|\mathcal{M}(e^+ \bar{u}_j \rightarrow \chi^+ \bar{u}_k)|^2 = \frac{\lambda'_{1jk}^2 g^2}{(\hat{s}^2 - m_{dk}^2)^2 + \Gamma_{dk}^2 m_{dk}^2} \epsilon_R^2 (\hat{s}^2 - \hat{s} m_{\chi^+}^2 - \hat{s} m_{u_k}^2) \quad (39)$$

where \hat{s}, t, u are defined by $\hat{s} = (p_e + p_{uj})^2 = xs$, $t = (p_e - p_{\chi^+})^2 = -Q^2$, $u = m_{\chi^+}^2 + m_{uk}^2 - \hat{s} - t$ and the coupling constants γ, δ, ϵ are

$$\begin{aligned}\gamma_L &= iV_{12}^* \quad , \quad \epsilon_R = -\frac{im_{dk}U_{12}}{\sqrt{2}M_W \cos \beta} \\ \delta_L &= \gamma_L \quad , \quad \delta_R = -\frac{im_{dj}U_{12}}{\sqrt{2}M_W \cos \beta}.\end{aligned}\quad (40)$$

We follow here the notation of [44], where one can find the expressions for the matrices U_{ij}, V_{ij} which diagonalise the chargino mass matrix.

10.3 Virtual Squark t-channel Exchange at LEP

The t-channel squark exchange contribution to the SM process $e^+e^- \rightarrow q\bar{q}$ can be obtained from [38] by crossing. The differential cross-section can then be expressed as

$$\frac{d\sigma(e^+e^- \rightarrow q\bar{q})}{d\cos\theta} = \frac{3}{32\pi s}(|A_1|^2 + |A_2|^2 + |A_3|^2) \quad (41)$$

and the amplitudes squared for the processes are given by

$$\begin{aligned}A_1 &= \frac{2e^4 Q_e^2 Q_q^2}{s^2} (t^2 + u^2) \\ &+ \frac{2g_Z^4}{|s - M_Z^2 + i\Gamma_Z M_Z|^2} [(v_e^2 + a_e^2)(v_q^2 + a_q^2)(t^2 + u^2) + 4v_e a_e v_q a_q (t^2 - u^2)] \\ &+ \mathcal{R}e\left\{\frac{1}{s - M_Z^2 + i\Gamma_Z M_Z}\right\} \frac{4Q_e Q_q e^2 g_Z^2}{s} [v_e v_q (t^2 + u^2) + a_e a_q (t^2 - u^2)] \\ A_2 &= \frac{\lambda_{1jk}^4}{2(t - \tilde{m}^2)^2} t^2 \\ A_3 &= \frac{-2\lambda_{1jk}^2 t^2}{t - \tilde{m}^2} \left(\frac{e^2 Q_e Q_q}{s} + \mathcal{R}e\left\{\frac{g_Z^2 (v_e v_q + a_e a_q)}{s - M_Z^2 + i\Gamma_Z M_Z}\right\} \right)\end{aligned}\quad (42)$$

where \tilde{m} is the mass of the exchanged squark, $g_Z = \frac{e}{\sin\theta_w \cos\theta_w}$

References

- [1] H1 Collaboration; “Observation of Events at very high Q^2 in ep Collisions at HERA”; DESY 97-24; submitted to Z.Phys. C.
- [2] ZEUS Collaboration; J.Breitweg et al.; “Comparison of ZEUS Data with Standard Model Predictions for $e^+ p \rightarrow e^+ X$ Scattering at High x and Q^2 ”; DESY 97-025; submitted to Z.Phys. C.
- [3] S. L. Adler, IASSNS-HEP-97-12, hep-ph/9702378; D. Choudhury, and S. Raychaudhuri, CERN-TH-97-026, hep-ph/9702392.
- [4] P. Haberl and F. Schrempp, 2nd HERA Workeshop, DESY, Hamburg, 1991; U. Martyn in “Future Physics at HERA”, 3rd HERA Workshop, DESY, Hamburg, 1996.

- [5] N. Harnew, 1st HERA Workshop, DESY, Hamburg, 1987.
- [6] J.L. Hewett, Contributed to Proceedings of the 1990 Summer Study on High Energy Physics, Snowmass, Colorado.
- [7] J. Butterworth, and H. Dreiner, Oxford Preprint OUNP-92-01, Oct 1991, publ. in Proc. of 2nd HERA Workshop on Physics, Hamburg, Germany, Oct 29-30, 1991.
- [8] J. Butterworth and H. Dreiner Nucl. Phys. B 397 (1993) 3.
- [9] E. Gildner, Phys. Rev. D 14 (1976) 1667; G. W. Anderson, and D. J. Castano, Phys.Rev. D 52 (1995) 1693.
- [10] For a review see for example H. E. Haber and G.L. Kane, Phys. Rept. 117 (1985) 75.
- [11] L.J. Hall and M. Suzuki, Nucl. Phys. B 231 (1984) 419.
- [12] S. Weinberg, Phys. Rev. D 26 (1982) 287; N. Sakai and T. Yanagida Nucl. Phys. B 197 (1982) 83; S. Dimopoulos, S. Raby and F. Wilczek, Phys. Lett. B 212 (1982) 133.
- [13] A. Yu. Smirnov, and F. Vissani, Phys. Lett. B 380 (1996) 317; J.L. Goity, and Marc Sher, Phys. Lett. B 346 (1995) 69, *ibid.* B 385 (1996) 500.
- [14] A. Chamseddine and H. Dreiner, Nucl. Phys. B 458 (1996) 65.
- [15] For example: D. E. Brahm, L. J. Hall, Phys. Rev. D 40 (1989) 2449, L. E. Ibanez, G. G. Ross, Nucl. Phys. B 368 (1992) 3; A. Yu. Smirnov, F. Vissani, Nucl. Phys. B 460 (1996) 37; A.H. Chamseddine, H. Dreiner, Nucl. Phys. B 447 (1995) 195.
- [16] H. Dreiner, and P. Morawitz, Nucl. Phys. B 428 (1994) 31.
- [17] T. Kon, K. Nakamura, T. Kobayashi, Z.Phys.C45:567,1990; Acta Phys. Polon. B21 (1990) 315; T. Kon, T. Kobayashi Phys.Lett.B270:81-88,1991; T. Kon, T. Kobayashi, S. Kitamura, K. Nakamura, S. Adachi Z.Phys.C61:239-246,1994; T. Kon, T. Kobayashi, S. Kitamura Phys. Lett. B 333 (1994) 263; T. Kobayashi, S. Kitamura, T. Kon, Int. J. Mod. Phys. A11 (1996) 1875.
- [18] E. Perez, Ph. D. Thesis, Universite de Paris, 1996.
- [19] H. Dreiner, E. Perez and Y. Sirois, Future Physics at HERA, 3rd HERA Workshop, DESY Hamburg, Sept. 1996.
- [20] M. Hirsch, H.V. Klapdor-Kleingrothaus, and S.G. Kovalenko, Phys. Rev. Lett. 75 (1995) 17; Phys. Rev. D 53 (1996) 1329.
- [21] V. Barger, G.F. Giudice, and T. Han, Phys. Rev. D 40 (1989) 2987.
- [22] S. Davidson, D. Bailey, B. A. Campbell, Z. Phys. C 61 (1994) 613.

- [23] P. Langacker, Phys Lett B256 (1991) 277.
- [24] R. M. Godbole, P. Roy, and X. Tata (Hawaii U.), Nucl. Phys. B 401 (1993) 67.
- [25] D.P. Roy, Phys. Lett. B 283 (1992) 270.
- [26] We have extracted this number from the tables in [1, 2].
- [27] H. Dreiner and G.G. Ross, Nucl. Phys. B 365 (1991) 597.
- [28] A.D. Martin, R.G. Roberts, W.J. Stirling; Phys. Lett. B 354(1995) 155; RAL/95-021(95).
- [29] J. Ellis and S. Rudaz, Phys. Lett. B 128 (1983) 248.
- [30] This field has been extensively studied recently, as an example consider P. Ramond, R.G. Roberts, G.G. Ross, Nucl. Phys. B 406 (1993) 19, and references therein.
- [31] M. Gluck, E. Reya, and A. Vogt, Z. Phys. C 67 (1995) 433.
- [32] A.Bartl,H.Fraas,W.Majerotto, Z.Phys.C(1987) 411.
- [33] H. Dreiner, J. Ellis, D.V. Nanopoulos, N.D. Tracas, and N.D. Vlachos, Mod. Phys. Lett. 3A (1988) 443.
- [34] D. Choudhury, Phys. Lett. B376(1996)201.
- [35] M. Carena, G.F. Giudice, S. Lola, C.E.M. Wagner, preprint CERN-TH-96-352.
- [36] ALEPH Collaboration, D. Buskulic et al., Phys. Lett.B 388 (1996) 419.
- [37] H1 Collaboration; Z.Phys. C71(1996)211.
- [38] W. Buchmuller, R. Ruckl, and D. Wyler, Phys. Lett. B 191 (1987) 442.
- [39] Seminar presented at CERN, February, 1997.
- [40] J. Hewett and S. Pakvasa, Phys. Rev. D 37 (1988) 3165.
- [41] d0 first generation lq-search; http://www-d0.fnal.gov/public/new/lq/lq_blurb.html
- [42] W. Beenakker, R. Hopker, M. Spira, and P. M. Zerwas, Phys. Rev. Lett. 74 (1995) 2905.
- [43] H. Dreiner, S. Lola, P. Morawitz; Phys. Lett. B 389 (1996) 62.
- [44] J.F. Gunion, H.E. Haber; Nucl. Phys. B 272 (1986) 1.